# Colocalized Delivery of Rapamycin and Paclitaxel to Tumors Enhances Synergistic Targeting of the PI3K/Akt/mTOR Pathway

Elvin Blanco[1], Takafumi Sangai[2], Suhong Wu[1], Angela Hsiao[1], Guillermo U Ruiz-Esparza[1,3], Carlos A Gonzalez-Delgado[1,3], Francisca E Cara[1], Sergio Granados-Principal[4], Kurt W Evans[2,5], Argun Akcakanat[2], Ying Wang[6], Kim-Anh Do[7], Funda Meric-Bernstam[2,5] and Mauro Ferrari[1]

*[1]Department of Nanomedicine, The Houston Methodist Research Institute, Houston, Texas, USA; [2]Department of Surgical Oncology, University of Texas, MD Anderson Cancer Center, Houston, Texas, USA; [3]Escuela de Biotecnología y Alimentos y Escuela de Medicina, Instituto Tecnológico y de Estudios Superiores de Monterrey, Monterrey, Mexico; [4]Houston Methodist Cancer Center, Houston Methodist Hospital, Houston, Texas, USA; [5]Department of Investigational Cancer Therapeutics, University of Texas MD Anderson Cancer Center, Houston, Texas, USA; [6]Department of Bioinformatics and Computational Biology, University of Texas MD Anderson Cancer Center, Houston, Texas, USA; [7]Department of Biostatistics, University of Texas, MD Anderson Cancer Center, Houston, Texas, USA*

Ongoing clinical trials target the aberrant PI3K/Akt/mammalian target of rapamycin (mTOR) pathway in breast cancer through administration of rapamycin, an allosteric mTOR inhibitor, in combination with paclitaxel. However, synergy may not be fully exploited clinically because of distinct pharmacokinetic parameters of drugs. This study explores the synergistic potential of site-specific, colocalized delivery of rapamycin and paclitaxel through nanoparticle incorporation. Nanoparticle drug loading was accurately controlled, and synergistic drug ratios established *in vitro*. Precise drug ratios were maintained in tumors 48 hours after nanoparticle administration to mice, at levels twofold greater than liver and spleen, yielding superior antitumor activity compared to controls. Simultaneous and preferential *in vivo* delivery of rapamycin and paclitaxel to tumors yielded mechanistic insights into synergy involving suppression of feedback loop Akt phosphorylation and its downstream targets. Findings demonstrate that a same time, same place, and specific amount approach to combination chemotherapy by means of nanoparticle delivery has the potential to successfully translate *in vitro* synergistic findings *in vivo*. Predictive *in vitro* models can be used to determine optimum drug ratios for antitumor efficacy, while nanoparticle delivery of combination chemotherapies in preclinical animal models may lead to enhanced understanding of mechanisms of synergy, ultimately opening several avenues for personalized therapy.

*Received 7 April 2013; accepted 13 February 2014; advance online publication 1 April 2014. doi:10.1038/mt.2014.27*

## INTRODUCTION

The phosphatidylinositol 3-kinase (PI3K)/Akt/mammalian target of rapamycin (mTOR) (PI3K/Akt/mTOR) pathway was found to be aberrantly activated in breast cancer, making inhibitors of PI3K, Akt, and mTOR powerful candidates for molecular-targeted therapy.[1–3] Consequently, the antitumor properties of rapamycin (RAP), a macrolide antibiotic and potent mTOR inhibitor, were extensively explored preclinically and clinically in breast cancer.[4] While antiproliferative effects were observed preclinically, especially in breast tumors with elevated levels of phosphorylated Akt and overexpressed S6K,[5] these results were largely cytostatic, leading to disease stabilization rather than regression in a clinical setting.[6,7] Synergy between rapamycin and several established chemotherapeutics was explored, with notable efficacy enhancement observed with paclitaxel (PTX),[8,9] although the precise mechanism of synergy was not thoroughly elucidated *in vitro*, and never demonstrated *in vivo*. Furthermore, clinically combining rapamycin analogues with paclitaxel has yielded modest response rates in patients.[10]

Several pharmacological obstacles limit the successful clinical translation of efficacious synergistic findings observed *in vitro*. Chemotherapeutics and drugs are formulated differently and administered to patients via distinct routes. Rapamycin analogs, such as everolimus (trade name: Afinitor), are available for oral ingestion,[6] while paclitaxel is administered intravenously as a Cremophor EL formulation (trade name: Taxol) or in an albumin-bound nanoparticle form (trade name: Abraxane).[11] The widely disparate pharmacokinetic parameters of each drug may very well preclude their coexistence in tumors. The question thus remains as to whether there is sufficient crosstalk between the effects of two synergistic drugs to elicit an efficacious response. Significant synergy observed *in vitro* may simply not effectively translate *in vivo* because of drug transport differentials and dissimilar tumor

*The first two authors contributed equally to this work and the last two authors share senior authorship.*

***Correspondence:*** *Mauro Ferrari, Department of Nanomedicine, The Houston Methodist Research Institute, 6670 Bertner St., M.S. R2-216, Houston, Texas 77030, USA. E-mail: mferrari@tmhs.org*

*Funda Meric-Bernstam, Department of Investigational Cancer Therapeutics, The University of Texas MD Anderson Cancer Center, 1400 Pressler Street, Unit 455, Houston, Texas 77030, USA. E-mail: fmeric@mdanderson.org*

residence times, hampering prospective benefits from combination therapies.

Our objective was to examine the therapeutic potential of delivering rapamycin and paclitaxel preferentially to breast tumors using nanoparticles. Nanomedicine platforms enable efficacious delivery of drugs by providing prolonged blood residence times through evasion of the reticuloendothelial system (RES), and by dramatically improving tumor accumulation of drugs through the enhanced permeability and retention effect.[12–14] Nanoparticle delivery of rapamycin and paclitaxel was hypothesized to result in superior therapeutic efficacy by providing a "same time, same place" scenario for drug synergy (**Supplementary Figure S1**). Polymer micelles,[15] core-shell nanoparticles formed from poly(ethylene glycol)-poly(ε-caprolactone) block copolymers, were used as drug carriers given their biocompatibility and lack of adverse effects.[16] Synergy following nanoparticle delivery was shown to be ratio-dependent both *in vitro* and *in vivo*, due to heightened delivery of both rapamycin and paclitaxel preferentially to tumors and precise preservation of drug ratios for extended time periods. Importantly, valuable mechanistic insights into rapamycin and paclitaxel synergy were observed *in vivo*, with combination therapy shown to affect Akt signaling through feedback loop inhibition, which is the first detailed proteomic examination of this mechanism.

## RESULTS

### Rapamycin and paclitaxel nanoparticles are small in size and encapsulate precise ratios of drugs efficiently and reproducibly

Nanoparticles were spherical and highly monodisperse (**Figure 1a**, **Supplementary Figure S2**) averaging 9.2 ± 3.8 nm in diameter as determined by dynamic light scattering (**Figure 1b**), with minimal variability between distinct formulations of rapamycin, paclitaxel, or coencapsulated nanoparticles (**Supplementary Figure S3**). Precise control of drug loading in the initial feed resulted in several reproducible formulations of varying ratios of rapamycin and paclitaxel within nanoparticles (**Figure 1c**). Release kinetics of both drugs from nanoparticles containing a 3:1 ratio of rapamycin and paclitaxel were diffusion-based and biphasic, with the majority (>80%) of drugs being released over the course of 24 hours (**Figure 1d**). Nanoparticles were found to be stable for prolonged periods of time in physiological media, as demonstrated by dynamic light scattering and atomic force microscopy analysis (**Supplementary Figure S3**).

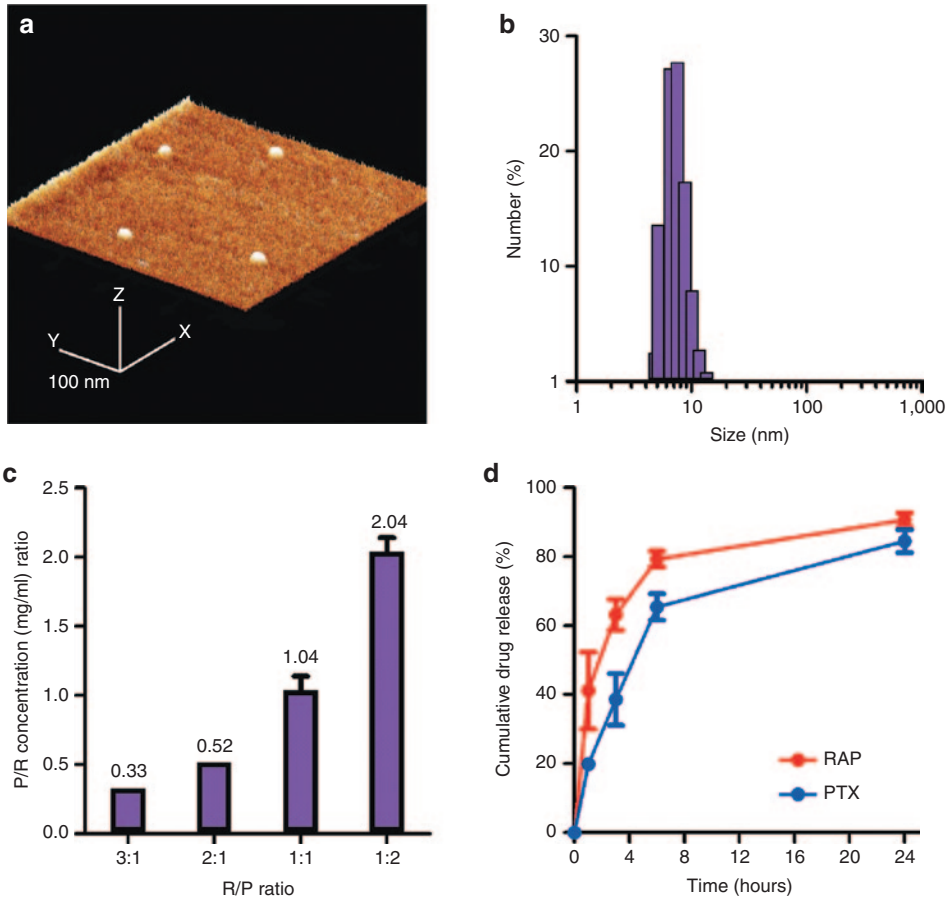


**Figure 1 Rapamycin and paclitaxel nanoparticles were monodisperse, small in size, and loaded drugs in precise ratios.** (**a**) Atomic force microscopy image of nanoparticles. The scale bar represents 100 nm. (**b**) Histogram depicting nanoparticle size as determined by dynamic light scattering. (**c**) Different loading ratios within nanoparticles explored, demonstrating consistency, reproducibility, and precision of drug loading. (**d**) *In vitro* release of rapamycin and paclitaxel from nanoparticles in phosphate-buffered saline at pH 7.4 and 37 °C. Results are shown as mean ± SEM.

## Drug-containing nanoparticles synergistically inhibit breast cancer growth *in vitro* in a ratio-dependent fashion

Varying ratios of rapamycin and paclitaxel were packaged within nanoparticles and administered to MDA-MB-468 and MCF-7 breast cancer cells in hopes of determining the most efficacious drug combination for synergy (**Figure 2**). Combination index analysis was performed based on dose-effect levels from median-effect plots of rapamycin nanoparticles alone, paclitaxel nanoparticles alone, and nanoparticles containing both drugs (**Figure 2a**). As stipulated by the method of Chou and Talalay, a combination index value of much less than 1 represents drug synergy, while a value closer to 1 indicates additive effects.[17] Enhanced synergy was more evident in nanoparticles containing drug ratios weighed more toward rapamycin than paclitaxel. Formulations where drugs were found in equal parts within the nanoparticle proved to be less synergistic, having an $ED_{50}$ combination index of 0.35 and 0.39 in MDA-MB-468 and MCF-7 cells, respectively. In contrast, a 3:1 ratio of rapamycin:paclitaxel was determined to be the most suitable for exploiting drug synergy in both MDA-MB-468 and MCF-7 cells, having $ED_{50}$ values of 0.10 and 0.19, respectively. **Figure 2b,c** represent growth inhibition plots of MDA-MB-468 and MCF-7 cells, respectively, treated with nanoparticles containing a 3:1 ratio of rapamycin and paclitaxel. Minimal difference with regards to cell growth inhibition was observed between free drug and nanoparticle formulations of rapamycin and paclitaxel (**Supplementary Figure S4**). Paclitaxel had a nominal impact on growth inhibition at lower doses, proving highly efficacious only at higher doses in both free and nanoparticle form. Given that MDA-MB-468 and MCF-7 cells were rapamycin-sensitive,[5,9,18] rapamycin and combination nanoparticles proved more effective at inhibiting breast cancer cell growth compared to paclitaxel nanoparticles alone at low doses. At the 10 ng/ml dose of rapamycin (3.3 ng/ml paclitaxel), combination nanoparticles were much more effective at inhibiting cell growth than single loaded nanoparticles ($P < 0.001$) in both cell lines, highlighting drug synergy at higher combination doses. In light of the efficacy of a 3:1 rapamycin:paclitaxel-containing nanoparticle, this ratio was selected for *in vivo* efficacy validation.

## Nanoparticles accumulate readily in tumors compared to liver and spleen, and preserve precise ratios of drugs intratumorally

The ability of nanoparticles to deliver rapamycin and paclitaxel preferentially to tumors was central to hypothesized synergy

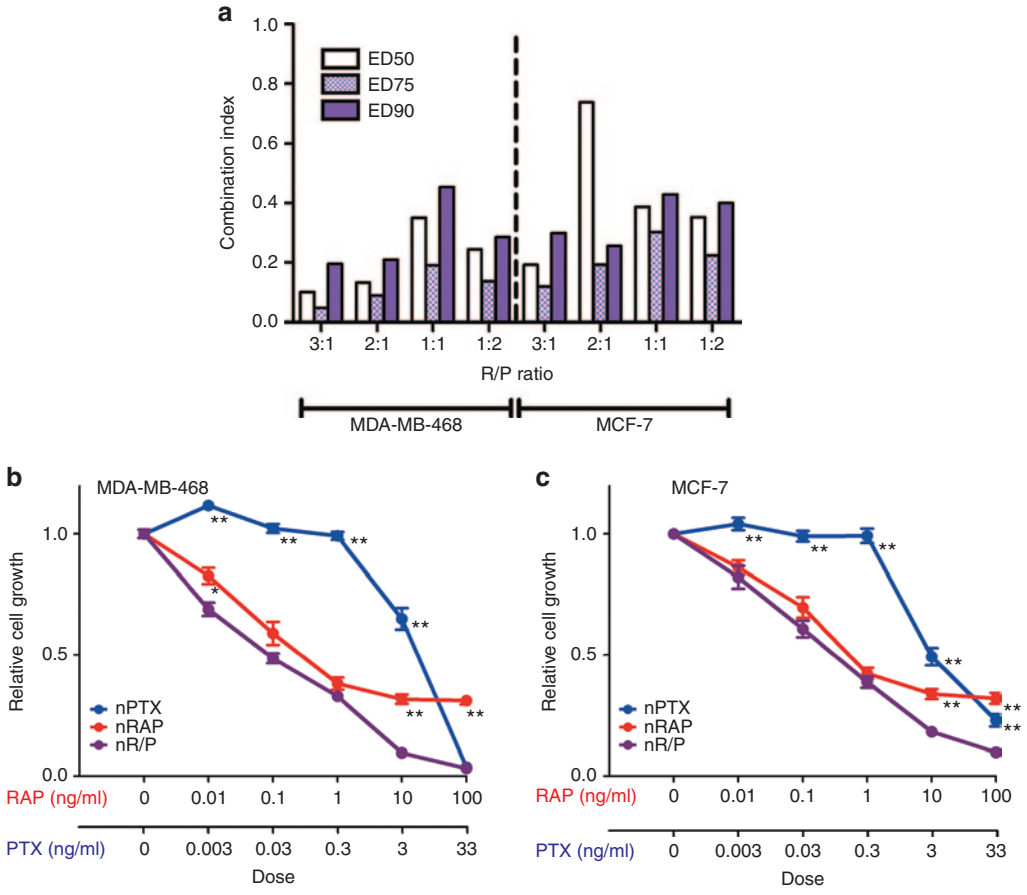


**Figure 2 Rapamycin and paclitaxel nanoparticles inhibit breast cancer cell growth *in vitro* in a ratio-dependent fashion.** (**a**) Combination index analysis of rapamycin and paclitaxel nanoparticles. Combination index values were calculated from growth inhibition assays and analyzed using the Chou and Talalay method.[17] (**b**) and (**c**) represent growth inhibition assays of MDA-MB-468 and MCF-7 breast cancer cells, respectively, treated with paclitaxel nanoparticles (nPTX), rapamycin nanoparticles (nRAP), and nanoparticles containing both rapamycin and paclitaxel (nR/P) at a 3:1 ratio of RAP:PTX. Asterisks denote data points where the difference was statistically significant when compared with R/P nanoparticles (*$P < 0.05$, **$P < 0.001$). All results are shown as mean ± SEM.

enhancement. Rapamycin and paclitaxel nanoparticles (nR/P) were administered to mice bearing MDA-MB-468 tumors and drug levels determined using liquid chromatography/tandem mass spectrometry (Figure 3). Both drugs were present in plasma at timepoints of 24 and 48 hours after intravenous administration (Figure 3a). When rapamycin and paclitaxel were administered via different routes of administration, and in different preparations, the accumulation of drugs in tumors varied significantly (Figure 3b–d). Delivery of both rapamycin in dimethyl sulfoxide intraperitoneally and paclitaxel Cremephor EL intravenously

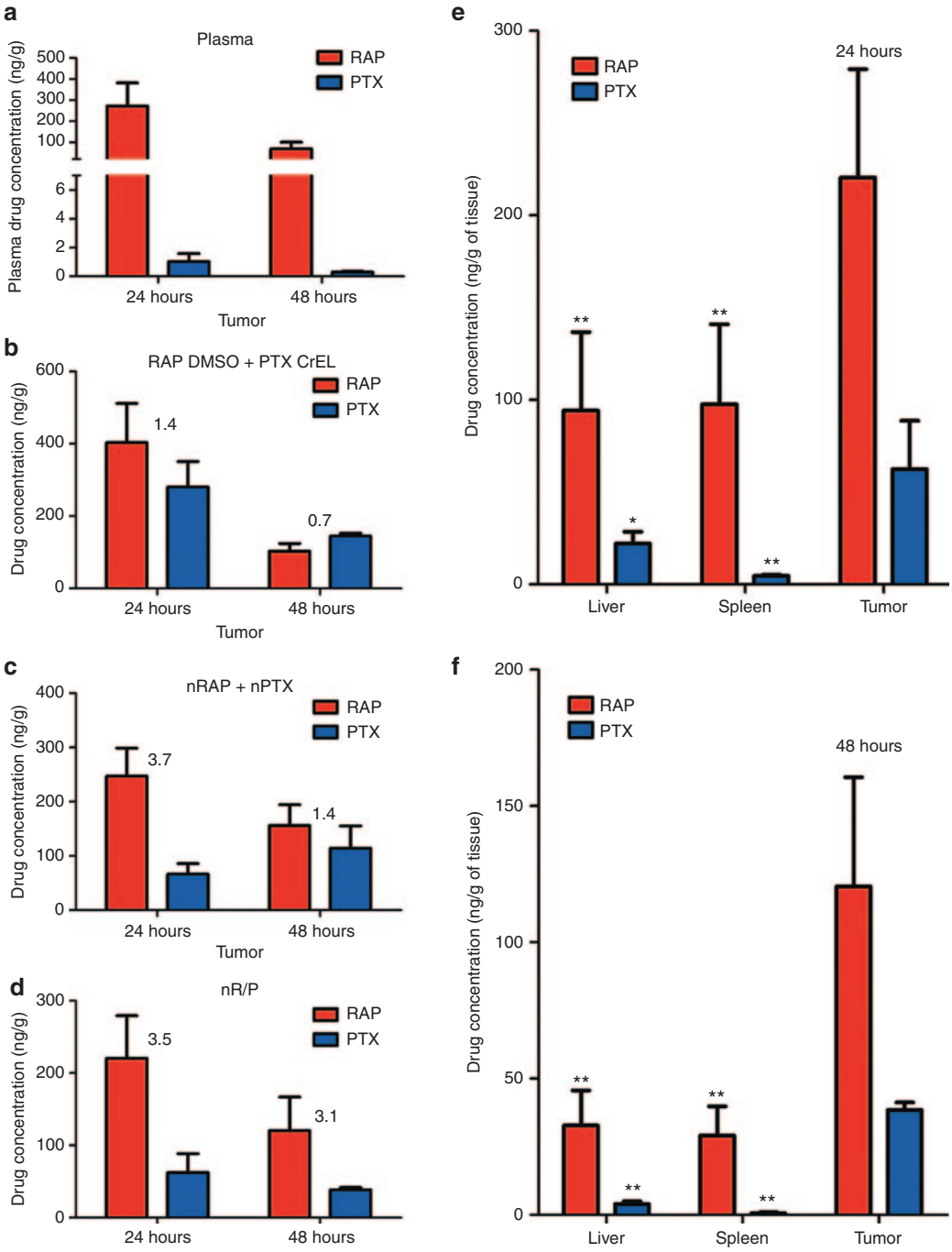


**Figure 3 Rapamycin and paclitaxel nanoparticles showed sustained presence in plasma, precisely preserved ratios in tumors, and accumulated to a larger extent in tumors than in organs comprising the reticuloendothelial system.** (**a**) Concentrations of rapamycin and paclitaxel were determined in plasma 24 and 48 hours after intravenous administration of nanoparticles (nR/P) containing a ratio of 3:1 rapamycin:paclitaxel (15:5 mg/kg). Rapamycin and paclitaxel amounts were examined in MDA-MB-468 tumors following administration of formulations consisting of: free rapamycin (RAP dimethyl sulfoxide) intraperitoneally and free paclitaxel (PTX CrEL) intravenously (**b**); individual nanoparticles administered intravenously as a physically mixed cocktail (nRAP+nPTX) (**c**); and coencapsulated rapamycin and paclitaxel nanoparticles (nR/P) administered intravenously (**d**), all at a dose of 15:5 mg/kg rapamycin:paclitaxel (3:1 ratio of rapamycin:paclitaxel). Concentrations of drugs were determined in liver, spleen, and tumor tissues of mice receiving coencapsulated rapamycin and paclitaxel nanoparticles (nR/P) at timepoints of (**e**) 24 and (**f**) 48 hours. Results are shown as mean ± SEM ($n = 3$). Statistical analysis was performed after normalization using liver concentrations (*$P < 0.05$; **$P < 0.01$ versus tumor).

was unable to preserve the 3:1 rapamycin:paclitaxel ratio. At 24 hours, the ratio of rapamycin:paclitaxel was 1.4, while at 48 hours, the paclitaxel amount was greater than rapamycin, and the ratio became 0.72. As another point of comparison, rapamycin and paclitaxel were loaded within individual nanoparticle formulations (nRAP, nPTX), mixed together in solution as a drug cocktail, and administered intravenously to mice (**Figure 3c**, **Supplementary Figure S5**). Interestingly, ratios of 3.7 and 1.4 at 24 and 48 hours, respectively, were observed in tumors excised from mice receiving a mixture of single-loaded nanoparticles. Of significant note, a precise ratio (3:1 rapamycin: paclitaxel) was preserved in tumors at the aforementioned timepoints when both drugs were copackaged within the same nanoparticle (**Figure 3d**). The rapamycin:paclitaxel concentration ratio at 24 hours was ~3.5, while at 48 hours, the ratio was ~3.2. Nanoparticles prepared at a different ratio of 1:2 rapamycin:paclitaxel were administered to tumor-bearing mice, and at 24 hours, a concentration ratio of 0.48 was observed in tumors, while a ratio of 0.39 was observed in tumors containing a mixture of nanoparticles (**Supplementary Figure S6**).

Concentrations of drugs in tumors were compared to those in the liver and spleen (**Figure 3e-f**), as these organs form part of the RES system, a system of monocytes and macrophages tasked with sequestering foreign materials from the bloodstream.[19] A more than twofold higher concentration of rapamycin was found in tumors compared to liver and spleen at 24 hours (220.5 ± 59 ng/g in tumors compared to 94.3 ± 42.5 and 97.7 ± 43.4 ng/g in liver and spleen, respectively) in mice receiving nanoparticles. This same trend of higher drug accumulation in tumors than RES organs was also observed when individual nanoparticle formulations were administered to mice (**Supplementary Figure S5**), as well as in a separate study involving nanoparticles with a 1:2 rapamycin:paclitaxel ratio (**Supplementary Figure S6**).

## Rapamycin and paclitaxel nanoparticles effectively suppress tumor growth *in vivo* and demonstrate that synergistic enhancement is the result of Akt feedback loop inhibition

Enhanced delivery of rapamycin and paclitaxel to tumors translated to pronounced antitumor efficacy *in vivo*. **Figure 4a** shows the antitumor response of dual-loaded nanoparticles in nude mice bearing MDA-MB-468 tumors. Paclitaxel Cremophor EL, a polyethoxylated castor oil formulation of PTX, was unable to successfully inhibit tumor growth at a concentration of 5 mg/kg. Paclitaxel nanoparticles alone initially proved ineffective, but gradually resulted in tumor growth inhibition by the end of the study. Rapamycin nanotherapeutics proved to be very effective at inhibiting tumor growth *in vivo*, at both low (1.5 mg/kg) and high doses (15 mg/kg), primarily due to the rapamycin-sensitive nature of the cell line. By day 10, tumors receiving rapamycin nanoparticles at doses of 1.5 and 15 mg/kg measured 476 ± 58 and 451 ± 53 $mm^3$, respectively. This efficacious response was sustained at both doses, resulting in tumors measuring 447 ± 59 and 471 ± 55 $mm^3$, respectively, by the end of the study. As hypothesized, nanoparticles containing both rapamycin and paclitaxel were highly efficacious *in vivo*, with regression observed immediately after the start of treatment. By day 10, tumors had regressed from a volume of 475 ± 75 to 357 ± 61 $mm^3$. This contrasts significantly from control tumors, which by this timepoint had an aforementioned volume of 744 ± 106 $mm^3$ ($P < 0.001$). By the end of the study, tumors had regressed to a volume of 301 ± 34 $mm^3$, compared to controls who had a volume of 1,015 ± 166 $mm^3$ ($P < 0.001$). In a separate antitumor efficacy study, PTX CrEL was administered intravenously along with an intraperitoneal injection of rapamycin in free drug form (dimethyl sulfoxide), and while tumor growth suppression was observed with respect to controls, the combination of drugs in free form proved less efficacious than nanoparticles encapsulating both rapamycin and paclitaxel (**Supplementary Figure S7**). Concomitant administration of individual nanoparticle formulations of rapamycin and paclitaxel also proved less effective at suppressing tumor growth than nanoparticles encasing both drugs within their core. Interestingly, while different doses and formulations of rapamycin (*i.e.*, 1.5 versus 15 mg/kg) resulted in tumor growth inhibition, the paclitaxel amount in nanoparticles was found to be important for tumor regression. Examination of tumor growth following administration of rapamycin and paclitaxel nanoparticles at a ratio of 3:1 and at a dose of 1.5:0.5 mg/kg did not result in a similar tumor growth inhibition pattern observed following administration of a 15:5 mg/kg dose (**Supplementary Figure S7**). An antitumor efficacy study in mice bearing MCF-7 breast tumors showed a similar trend of tumor regression following administration of a 3:1 ratio of rapamycin to paclitaxel, and this regression was more pronounced than responses observed with a 1:2 ratio of RAP:PTX, a ratio found to be synergistically inferior to the 3:1 ratio *in vitro* (**Supplementary Figure S8**).

Reverse-phase protein array (RPPA) analysis was conducted on excised tumors from treated mice to determine the effects of combination therapy on the PI3K/Akt/mTOR pathway (**Figure 4b**). Low-dose rapamycin nanoparticle treatment significantly inhibited mTOR downstream signaling, decreasing phosphorylation on pS6K T389, pS6 S235/236, and pS6 S240/244 ($P < 0.0001$, $P = 0.0002$, and $P = 0.0001$, false discovery rate (FDR) < 0.1 respectively), and at the same time, significantly increasing Akt phosphorylation on pAkt T308 and pAkt S473 ($P = 0.0121$ and $P = 0.0144$, FDR < 0.2), a previously described feedback loop activation.[20–22] Moreover, the Akt downstream target of pBad S112 was also significantly increased ($P = 0.0027$, FDR < 0.1). Low-dose paclitaxel nanoparticles did not show any statistical effect on the PI3K/Akt/mTOR pathway (**Supplementary Table S1**). Upon comparison among the four groups, including control, low-dose paclitaxel nanoparticles, high-dose rapamycin nanoparticles, and combination nanoparticles, high-dose rapamycin nanoparticle treatment led to significant decreases in pS6K T389, pS6 S235/236, and pS6 S240/244 ($q = 0.00676$, $q = 0.00112$, and $q = 0.00124$, respectively) (**Supplementary Table S2**). Similarly, a decrease in pS6 S235/236 immunostaining was observed by immunohistochemistry (**Figure 4c**). In contrast, pAkt T308, pAkt S473, and phosphorylation of Akt's target pBad S112 were significantly increased ($q = 0.01963$, $q = 0.06055$, and $q = 0.06055$, respectively) following rapamycin nanoparticle treatment. Downstream Akt targets pGSK3 βS9 and pPRAS40 T246 were also increased following rapamycin nanoparticle treatment ($q = 0.06895$ and $q = 0.07511$). Interestingly, the combination of rapamycin and

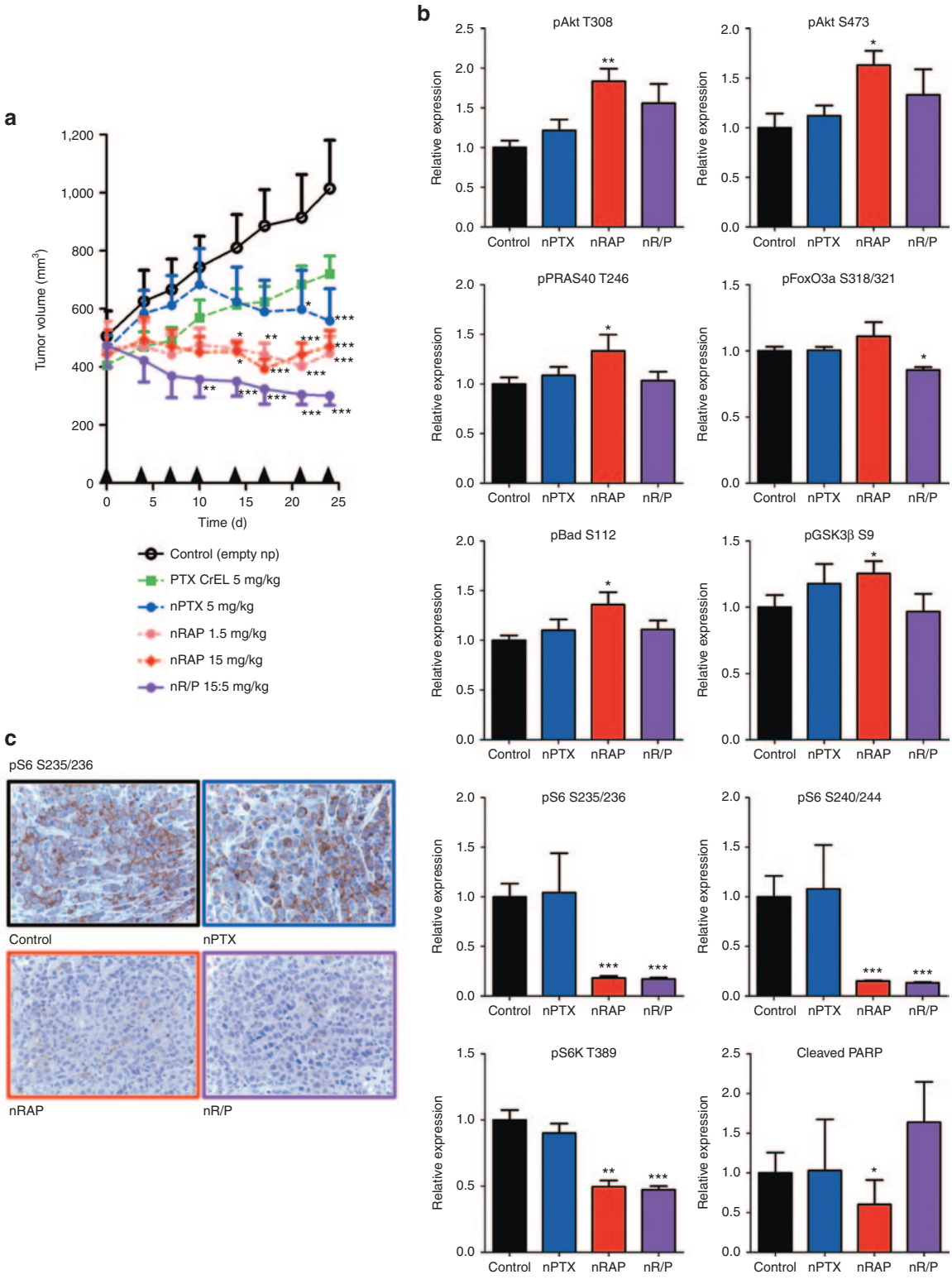


**Figure 4 Rapamycin and paclitaxel nanoparticles suppressed tumor growth *in vivo*, acting specifically on key molecular targets of the PI3K/Akt/mTOR pathway.** (**a**) Tumor growth inhibition following administration of individual rapamycin and paclitaxel nanoparticles (nRAP, nPTX) and nanoparticles containing both drugs (nR/P) to mice bearing MDA-MB-468 tumors (mean ± SEM, $n = 5$). Arrows denote administration timepoints. Asterisks denote results that are statistically significant compared to the control group (*$P < 0.05$; **$P < 0.01$; ***, $P < 0.001$). (**b**) Relative expression of proteins involved in the PI3K/Akt/mTOR pathway as determined by reverse-phase protein array analysis of tumors excised 24 hours after treatment. The data are normalized by the value of the control and graphs are shown as mean ± SEM ($n = 5$). Asterisks represent statistical significance compared to control (*$q < 0.1$; **$q < 0.05$; ***$q < 0.005$). (**c**) pS6 S235/236 immunohistochemical staining of excised tumors 24 hours after administration of nanoparticles. The scale bar represents 20 μm.

paclitaxel nanoparticle treatment significantly inhibited S6K and S6 phosphorylation on pS6K T389, pS6 S235/236, and pS6 S240/244 ($q = 0.00151$, $q = 0.00139$, and $q = 0.00151$, respectively), but did not significantly increase pAkt T308 or pAkt S473 ($q = 0.31765$ and $q = 0.52404$) (**Supplementary Table S3**) compared to rapamycin nanoparticles. Rather than activate Akt, Akt downstream targets pp27 T157 and pFoxO3a S318/321 were significantly decreased ($q = 0.06132$ and $q = 0.06132$).

## DISCUSSION

Effective translation of synergy observed in properly controlled *in vitro* scenarios to the highly complex *in vivo* setting remains a formidable challenge in chemotherapy. We hypothesized that synergistic antitumor effects could be significantly increased if both drugs were delivered site specifically and simultaneously to tumors, through encapsulation within nanoparticles. Several nanoparticle platforms have emerged as viable drug delivery platforms in the clinical arena, and are now known to significantly reduce morbidity associated with conventional drug preparations such as cardiotoxicity and hypersensitivity reactions in the case of doxorubicin[23] and paclitaxel,[24] respectively.

Herein, rapamycin and paclitaxel nanoparticles inhibited breast cancer cell growth *in vitro*. Importantly, degree of synergy varied depending on the ratio of drugs within nanoparticles, demonstrating the importance in selecting not only the correct combination of drugs but also the correct amount. Nanoparticles containing drug ratios weighed more toward rapamycin, an antibiotic, than paclitaxel, a chemotherapeutic, were more effective at inhibiting tumor growth. These findings challenge the practice in chemotherapy where drugs are administered at concentrations approximating their maximum tolerated doses (MTDs). Increasing the concentration of one or both drugs to near-MTD levels may not serve any distinct therapeutic advantage and may possibly result in patient morbidity. As an example, a study involving patients with metastatic breast cancer receiving either 175, 210, or 250 mg/m$^2$ showed that higher doses of paclitaxel did not improve patient response rates or quality of life.[25] Our study suggests that combination therapies consisting of molecular-targeted agents and chemotherapeutics can be tailored accordingly based on *in vitro* predictive models of synergy to ensure maximal efficacy and reduced toxicity.

Rapamycin and paclitaxel were found in plasma at long time periods after administration of nanoparticles, likely the result of long-circulating half-lives of similar nanoparticles,[26,27] as well as possible drug binding to circulating plasma proteins, including human serum albumin, lipoprotein, and α, β, and γ globulins.[28–30] Increased blood residence times are important for tumor accumulation, given that multiple passes through tumor-associated vasculature increases the likelihood of permeating through fenestrated blood vessels via the enhanced permeability and retention effect.[31] Indeed, paclitaxel and rapamycin were found in excised tumors 48 hours after administration. This is likely due to the enhanced permeability and retention effect, as well as altered clearance and volume of distribution. Previously, a micellar formulation of paclitaxel with a twofold increase in volume of distribution and clearance compared to albumin-bound paclitaxel nanoparticles translated to improved responses.[32] In the present study, both drugs were found at higher levels in the tumor than in the liver and spleen, organs that comprise the RES. High tumor accumulation of drugs likely resulted from the small size of the nanoparticles (~10 nm). In a study by Lam and coworkers, doxorubicin micelles measuring 10 nm in diameter accumulated more in tumors at 16 hours postinjection than in the liver and spleen.[33] Porter and coworkers compared the biodistribution of doxorubicin liposomes (89 nm) and doxorubicin dendrimers (12 nm), showing that the latter resulted in significantly higher levels in tumor than in the spleen and liver when compared to the former, which was found to accumulate more in RES organs.[34] Higher accumulation of nanoparticles in tumors compared to healthy organs is expected to increase drug bioavailability, thereby enhancing efficacy while decreasing side effects.

Biodistribution results demonstrate that distinct ratios of drugs within nanoparticles were precisely preserved within tumors at timepoints of 24 and 48 hours, a result that was not possible with free drug preparations administered via separate routes or coadministration of individually formulated nanoparticles. Moreover, the most synergistic ratio observed *in vitro* was found to result in significant tumor growth inhibition in both MDA-MB-468 and MCF-7 tumors in mice. In MCF-7 breast tumors, a ratio proven to be more synergistic than another ratio *in vitro* (3:1 versus 1:2 rapamycin:paclitaxel) was indeed more efficacious at hindering tumor growth than that same ratio *in vivo*, extending the notion of "same time, same place" for synergy enhancement to include "specific amounts." The present study attempts to make a case for optimum chemotherapy by using *in vitro* synergistic analyses (*i.e.*, combination index analysis) to predict *in vivo* tumor responses.

Enhanced delivery of rapamycin and paclitaxel to tumors via nanoparticles provided valuable insights into the mechanism of synergy enhancement involving suppression of feedback loop Akt phosphorylation. Consequently, this led to inhibition of several downstream targets of Akt, including PRAS40, Bad, GSK3β, as well as S6K and S6, the downstream targets of mTOR. Synergy between rapamycin and paclitaxel has been explored preclinically in several different cancers,[9,35,36] and clinically in several completed[37,38] and ongoing trials, with the precise mechanism remaining elusive. The initial rationale for synergy was sound, with reports pointing to the role of mTOR as a cell survival protein[9] and Akt activation after paclitaxel treatment causing resistance to the drug.[39,40] However, rapamycin was also reported to activate Akt through negative feedback loop activation.[20–22] Results from our study indicate that pAkt is indeed increased following rapamycin treatment. However, coadministration of low-dose paclitaxel with rapamycin was not associated with a statistically significant increase in pAkt compared to rapamycin controls, and inhibited activation of PRAS40, itself an inhibitor of mTOR, and GSK3β, a key protein involved in cellular proliferation, as well as Bad and the FoxO family, proteins involved in apoptosis (**Figure 5**). One of the reasons for inhibition of Akt activation by paclitaxel is possibly related to nuclear translocation of FoxO3a by paclitaxel.[41] This is the first report that demonstrates inhibition of Akt activation following rapamycin and paclitaxel treatment *in vivo* by RPPA, proving detailed proteomic insights into mechanisms of synergy. As only one ratio was examined *in vivo*, it is not possible to state whether similar

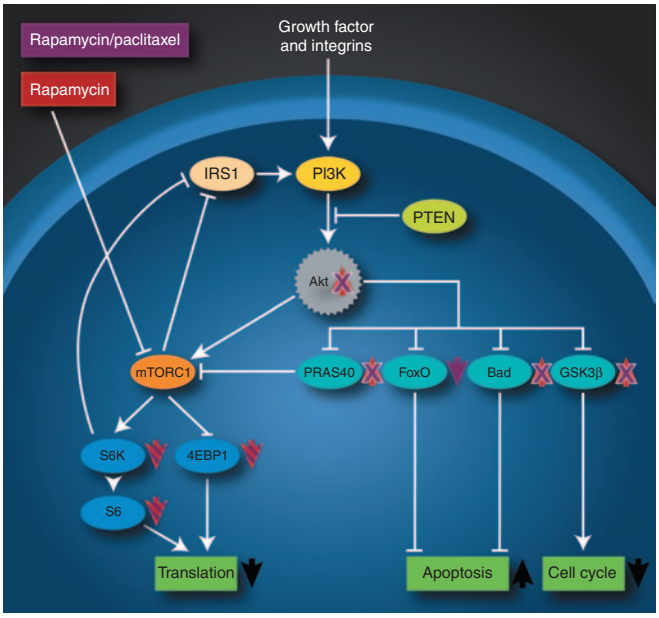


**Figure 5 Rapamycin and paclitaxel nanoparticles synergistically target the PI3K/Akt/mTOR pathway by suppressing feedback loop Akt phosphorylation.** Rapamycin nanoparticle treatment alone caused a decrease in phosphorylated S6 and S6K, as well as 4E-BP1, and an increase in pAkt through feedback loop activation. Rapamycin and paclitaxel delivered within the same nanoparticle also led to a decrease in phosphorylated S6, S6K, and 4E-BP1, but resulted in a decrease in pAkt. Combination therapy also inhibited phosphorylation of PRAS40, Bad, and GSK3β, all previously shown to increase with rapamycin treatment alone. Colocalized delivery of rapamycin and paclitaxel also showed a decrease in phosphorylation of FoxO proteins. Taken together, the effects of combination therapy led to synergistic enhancement of cell death by decreasing protein translation, increasing apoptosis, and decreasing cell cycle progression.

suppression of Akt phosphorylation would be observed with different ratios that may not have shown efficacious synergy *in vitro*, and it is entirely possible that a different mechanism may also be responsible for the synergistic effect observed. Drug synergy may not be fully realized in patients because of a lack of proper models to understand key molecular effectors and targets involved in synergy *in vivo*. These mechanistic insights may contribute towards a retooling of current chemotherapeutic regimens, or in establishing novel trials with rapamycin and molecular-targeted agents that act specifically on proteins such as Akt.[18]

We highlight the potential of nanotherapeutics for enabling preferential and simultaneous delivery of specific combinations of synergistic drugs. Synergy was ratio specific, with more pronounced antitumor effects observed in ratios containing less paclitaxel than rapamycin. Drugs accumulated in tumors at more elevated levels than in the liver and spleen, with precise ratios preserved for prolonged timepoints in tumors, translating proven *in vitro* synergistic potential to the *in vivo* setting. Nanoparticle delivery of rapamycin and paclitaxel in preclinical animal models shed further light on the mechanism of drug synergy involving inhibition of Akt feedback loop activation, the first report of this kind. The ability to use nanoparticle drug delivery to tailor chemotherapeutic regimens based on *in vitro* predictive models designed to maximize synergy and reduce side effects opens several avenues for personalized medicine.

## MATERIALS AND METHODS

***Materials.*** Poly(ethylene glycol)-block-poly(ε-caprolactone) ($M_n$ = 10,000 Da) was purchased from Sigma Aldrich (St Louis, MO). Rapamycin (RAP) and paclitaxel (PTX) were purchased from LC Laboratories (Woburn, MA). Paclitaxel Cremephor EL (PTX CrEL) was purchased from Teva Pharmaceuticals (Petach, Tikva, IL). All organic solvents were of analytical grade. Rapamycin-sensitive human breasts cancer cell lines MDA-MB-468 and MCF-7 were obtained from the American Tissue Culture Collection (Manassas, VA). Cell lines were cultured in Dulbecco's modified Eagle's medium (DMEM)/F-12 (Mediatech, Manassas, VA) supplemented with 10% (v/v) FBS (Sigma Aldrich). Cells were maintained at 37 °C in a humidified atmosphere containing 5% $CO_2$.

***Nanoparticle fabrication and characterization.*** A previously established solvent evaporation procedure was used to fabricate nanoparticles.[42] Nanoparticles were characterized for morphology and size using a MultiMode 8 Atomic Force Microscope (AFM) (Bruker AXS, Fitchburg, WI) in ScanAsyst-HR imaging mode in air using a silicon tip on nitride lever with a spring constant of 0.4 N/m. Nanoparticle size was characterized by transmission electron microscopy (TEM) using a JEM 1210 TEM (JEOL USA, Peabody, MA) at an accelerating voltage of 80 kV. Size measurements of all nanoparticle formulations were obtained using a Malvern Zetasizer Nano ZS dynamic light scattering (DLS) instrument (Malvern Instruments, Worcestershire, UK). RAP and PTX concentrations were determined via HPLC using modified versions of previously published methods.[43] Release kinetics of both drugs from nanoparticles were examined using a previously established procedure,[44] with amount of RAP and PTX released determined by HPLC as described above. Stability of different nanoparticle formulations over time was examined in FBS at 37 °C. Nanoparticles were removed from media at predetermined time points, after which DLS measurements of size were obtained and verified via AFM.

**In vitro *antitumor efficacy of RAP/PTX nanoparticles.*** Antiproliferative activity was tested in MCF-7 and MDA-MB-468 by sulforhodamine B (SRB) assays as described previously.[45] The median inhibitory concentration ($IC_{50}$) of each cell line was determined from dose–response curves for 4 days treatment by using Calcusyn software from Biosoft (Cambridge, UK). Dose–response curves yielded $IC_{50}$ values used in the calculation of the combination index by the method of Chou and Talalay.[17]

**In vivo *biodistribution evaluation in breast cancer.*** All animal experiments were approved by the MD Anderson Institutional Animal Care and Use Committee. MDA-MB-468 cells ($1 \times 10^7$ cells) were inoculated in the mammary fat pads of 4- to 6-week-old female nu/nu mice. Mice were euthanized 24 and 48 hours after administration, and liver, spleen, and tumors of the mice were harvested, weighed, and snap frozen in liquid nitrogen biodistribution analysis.

Biodistribution analysis was performed in The University of Texas MD Anderson Cancer Center Pharmacology and Analytical Laboratory Facility. For biodistribution analysis, mouse liver, spleen, and tumor homogenates were prepared in PBS. Drugs were extracted using a liquid-liquid method. Rapamycin and paclitaxel concentrations were determined by liquid chromatography/tandem mass spectrometry (LC-MS/MS). For rapamycin, a Waters Acquity UPLC system was used in tandem with a Waters Quattro Premier CE mass spectrometer using MassLynx/QuanLynx software for data acquisition and integration. Chromatographic separation was carried out on a Phenomenex Kinetex $C_{18}$ column (100 × 2.1 mm, 2.6 μm particle size). The mobile phase consisted of 0.2% formic acid in water (A) and methanol (B) and was delivered at 0.4 ml/minute in a gradient mode (time(minute)/%B): 0/40, 0.5/40, 1.5/98, 2.5/98, 3.5/40, and 5/40. Paclitaxel concentrations were determined using an Agilent 1100 series system in tandem with a Micromass Quattro Ultima mass spectrometer. Chromatographic separation was carried out on a Phenomenex Kinetex PFP column (50 × 2.1 mm, 2.6 μm particle size). Column temperature was

maintained at 60 °C. The mobile phase consisted of 0.2% formic acid in water (A) and acetonitrile (B) and was delivered at 0.35 ml/minute in a gradient mode (time(minute)/%B): 0/50, 0.25/50, 2.5/95, 3.0/95, 4.0/50, and 6/50. Rapamycin was monitored in the positive electrospray mode ($ESI^+$) at a mass transition 981 > 389, while paclitaxel at a mass transition 854 > 268. The retention time of rapamycin was 2.26 minutes and that of paclitaxel was 1.50 minutes. Calibration curves were constructed over the range from 1 to 500 ng/ml with correlation coefficients greater than 0.9964 for rapamycin, while those for paclitaxel were constructed over the range from 0.1 to 500 ng/ml with correlation coefficients greater than 0.9994.

**In vivo *antitumor efficacy analysis of RAP/PTX nanoparticles.*** For *in vivo* antitumor efficacy studies, MCF-7 ($5 \times 10^6$) and MDA-MB-468 cells ($1 \times 10^7$ cells) were inoculated in the mammary fat pads of female nu/nu mice. MCF-7 breast cancer cells were inoculated in mice previously implanted with 17β-estradiol pellets subcutaneously. Treatments were given intravenously twice-a-week for the duration of 4 weeks. Tumor size was monitored by caliper measurements and tumor volumes calculated as previously described.[9]

***RPPA and immunohistochemical analysis of tumors.*** RPPA analysis was performed in The University of Texas MD Anderson Cancer Center Functional Proteomics RPPA Core Facility as described previously.[46–48] To determine the effect of rapamycin and paclitaxel combinations *in vivo*, MDA-MB-468 tumors ($n = 5$) excised after efficacy studies were lysed in RPPA lysis buffer. Samples were probed with 154 monospecific, validated antibodies, enriched for components of the PI3K/Akt/mTOR pathway. Immunohistochemical analysis was performed on the same tumor samples used for RPPA analysis ($n = 5$ from each group). Epitope retrieval was carried out in citrate buffer (pH 6) for 20 minutes at 98 °C. Endogenous peroxidase activity was blocked by addition of 3% hydrogen peroxide. Dako protein serum was added to block nonspecific antibody binding. Anti pS6 S235/236 rabbit monoclonal antibody (Cell Signaling Technology, Danvers, MA) was diluted at 1:100 and incubated at room temperature for 30 minutes. Vector secondary antibody anti-rabbit HRP labeled was used and developed with diaminobenzidine.

***Statistical analysis.*** For *in vitro* studies, comparison between two, and multiple groups were performed by Student's *t*-test and one-way ANOVA, followed by Tukey's multiple comparison tests, respectively. For *in vivo* tumor efficacy studies, two-way ANOVA, followed by Bonferroni post-tests, was performed. To determine the effect of rapamycin and paclitaxel combination on proteins expression *in vivo*, the RPPA data were statistically analysed in R. Data were first normalized using median centering. Feature-by-feature two-sample *t*-tests were used for comparisons between two groups. The β-uniform mixture models were used to fit the resulting *P*-value distributions in order to adjust for multiple comparisons.[49] Cutoff *P* values and number of significant proteins were computed for FDR < 0.2. *q* Values represent FDR-adjusted *P* values for multiple comparisons.[50]

## SUPPLEMENTARY MATERIAL

**Figure S1.** the hypothesized mechanism of action behind nanoparticle delivery of synergistic drugs to breast tumors.

**Figure S2.** transmission electron microscopy (TEM) micrograph of rapamycin and paclitaxel nanoparticles, depicting their nanoscale size range (~9 nm), their core-shell architecture, and their monodispersity.

**Figure S3.** Nanoparticle size and surface charge did not vary significantly depending on formulation, and were stable for long periods of time in physiological media.

**Figure S4.** Nanoparticles containing both rapamycin and paclitaxel synergistically inhibited breast cancer cell growth in a manner analogous to free drug combinations in vitro.

**Figure S5.** Rapamycin and paclitaxel packaged individually in nanoparticles and coadministered to mice bearing MDA-MB-468 breast tumors had sustained presence in the blood, adequately accumulated in tumors, and maintained drug ratios at early timepoints.

**Figure S6.** Nanoparticles containing both rapamycin and nanoparticles at a ratio of 1:2 rapamycin:paclitaxel showed sustained presence in plasma, precisely preserved the ratio in tumors, and accumulated to a larger extent in tumors than in organs comprising the reticuloendothelial system.

**Figure S7.** Nanoparticles containing both rapamycin and paclitaxel effectively suppressed tumor growth inhibition in vivo compared to free drug and individual nanoparticle combination controls.

**Figure S8.** Synergistic ratios obtained from combination index analyses predicted in vivo antitumor efficacy in murine models of breast cancer.

**Table S1.** Differentially expressed proteins in control and paclitaxel nanoparticle 5 mg/kg treated tumor (FDR < 0.2).

**Table S2.** Differentially expressed proteins in control and rapamycin nanoparticle 15 mg/kg treated tumor (FDR < 2).

**Table S3.** Differentially expressed proteins in control vs rapamycin(15) + paclitaxel(5) nanoparticle treated tumor (FDR < 0.2).

## ACKNOWLEDGMENTS

We appreciate the assistance of James Barrish (Texas Children's Hospital) in conducting TEM; Dannette K. Doolittle, Edd Felix, and Q. Alan Xu (UT MD Anderson) for drug estimation levels in tissues; Raul A. Gonzalez (TMHRI) for immunohistochemistry; and Matthew G. Landry for manuscript schematics. This work was supported by a CDMRP Department of Defense Breast Cancer Research Program (DOD/BCRP) Innovator Award (grant number W81XWH-09-1-0212) awarded to M.F., a National Center for Research Resources NIH grant (UL1TR000371) to F.M.B. and Y.W., and a support grant from the University of Texas MD Anderson Cancer Center (P30 CA016672). Work was also supported by postdoctoral fellowships from DOD/BCRP (grant number W81XWH-11-1-0103) and the Susan G. Komen Breast Cancer Foundation (grant number KG101394) awarded to E.B. The authors declare no financial conflict of interest.

## REFERENCES

1. Calvo, E, Bolós, V and Grande, E (2009). Multiple roles and therapeutic implications of Akt signaling in cancer. *Onco Targets Ther* **2**: 135–150.
2. Carraway, H and Hidalgo, M (2004). New targets for therapy in breast cancer: mammalian target of rapamycin (mTOR) antagonists. *Breast Cancer Res* **6**: 219–224.
3. Meric-Bernstam, F and Gonzalez-Angulo, AM (2009). Targeting the mTOR signaling network for cancer therapy. *J Clin Oncol* **27**: 2278–2287.
4. Dancey, J (2010). mTOR signaling and drug development in cancer. *Nat Rev Clin Oncol* **7**: 209–219.
5. Noh, WC, Mondesire, WH, Peng, J, Jian, W, Zhang, H, Dong, J *et al.* (2004). Determinants of rapamycin sensitivity in breast cancer cells. *Clin Cancer Res* **10**: 1013–1023.
6. Ellard, SL, Clemons, M, Gelmon, KA, Norris, B, Kennecke, H, Chia, S *et al.* (2009). Randomized phase II study comparing two schedules of everolimus in patients with recurrent/metastatic breast cancer: NCIC Clinical Trials Group IND.163. *J Clin Oncol* **27**: 4536–4541.
7. Fleming, GF, Ma, CX, Huo, D, Sattar, H, Tretiakova, M, Lin, L *et al.* (2012). Phase II trial of temsirolimus in patients with metastatic breast cancer. *Breast Cancer Res Treat* **136**: 355–363.
8. Fung, AS, Wu, L and Tannock, IF (2009). Concurrent and sequential administration of chemotherapy and the Mammalian target of rapamycin inhibitor temsirolimus in human cancer cells and xenografts. *Clin Cancer Res* **15**: 5389–5395.
9. Mondesire, WH, Jian, W, Zhang, H, Ensor, J, Hung, MC, Mills, GB *et al.* (2004). Targeting mammalian target of rapamycin synergistically enhances chemotherapy-induced cytotoxicity in breast cancer cells. *Clin Cancer Res* **10**: 7031–7042.
10. Gonzalez-Angulo, AM, Green, MC, Murray, JL, Palla, SL, Koenig, KH, Brewster, AM *et al.* (2011). Open label, randomized clinical trial of standard neoadjuvant chemotherapy with paclitaxel followed by FEC (T-FEC) versus the combination of paclitaxel and RAD001 followed by FEC (TR-FEC) in women with triple receptor-negative breast cancer (TNBC). *J Clin Oncol* **29**: (suppl; abstr 1016).
11. Green, MR, Manikhas, GM, Orlov, S, Afanasyev, B, Makhson, AM, Bhar, P *et al.* (2006). Abraxane, a novel Cremophor-free, albumin-bound particle form of paclitaxel for the treatment of advanced non-small-cell lung cancer. *Ann Oncol* **17**: 1263–1268.
12. Davis, ME, Chen, ZG and Shin, DM (2008). Nanoparticle therapeutics: an emerging treatment modality for cancer. *Nat Rev Drug Discov* **7**: 771–782.
13. Ferrari, M (2005). Cancer nanotechnology: opportunities and challenges. *Nat Rev Cancer* **5**: 161–171.
14. Torchilin, V (2011). Tumor delivery of macromolecular drugs based on the EPR effect. *Adv Drug Deliv Rev* **63**: 131–135.
15. Cabral, H, Nishiyama, N and Kataoka, K (2011). Supramolecular nanodevices: from design validation to theranostic nanomedicine. *Acc Chem Res* **44**: 999–1008.
16. Zhao, B, Wang, XQ, Wang, XY, Zhang, H, Dai, WB, Wang, J *et al.* (2013). Nanotoxicity comparison of four amphiphilic polymeric micelles with similar hydrophilic or hydrophobic structure. *Part Fibre Toxicol* **10**: 47.

17. Chou, TC and Talalay, P (1984). Quantitative analysis of dose-effect relationships: the combined effects of multiple drugs or enzyme inhibitors. *Adv Enzyme Regul* **22**: 27–55.
18. Sangai, T, Akcakanat, A, Chen, H, Tarco, E, Wu, Y, Do, KA *et al.* (2012). Biomarkers of response to Akt inhibitor MK-2206 in breast cancer. *Clin Cancer Res* **18**: 5816–5828.
19. Peer, D, Karp, JM, Hong, S, Farokhzad, OC, Margalit, R and Langer, R (2007). Nanocarriers as an emerging platform for cancer therapy. *Nat Nanotechnol* **2**: 751–760.
20. Meric-Bernstam, F, Akcakanat, A, Chen, H, Do, KA, Sangai, T, Adkins, F *et al.* (2012). PIK3CA/PTEN mutations and Akt activation as markers of sensitivity to allosteric mTOR inhibitors. *Clin Cancer Res* **18**: 1777–1789.
21. O'Reilly, KE, Rojo, F, She, QB, Solit, D, Mills, GB, Smith, D *et al.* (2006). mTOR inhibition induces upstream receptor tyrosine kinase signaling and activates Akt. *Cancer Res* **66**: 1500–1508.
22. Sun, SY, Rosenberg, LM, Wang, X, Zhou, Z, Yue, P, Fu, H *et al.* (2005). Activation of Akt and eIF4E survival pathways by rapamycin-mediated mammalian target of rapamycin inhibition. *Cancer Res* **65**: 7052–7058.
23. O'Brien, ME, Wigler, N, Inbar, M, Rosso, R, Grischke, E, Santoro, A *et al.*; CAELYX Breast Cancer Study Group. (2004). Reduced cardiotoxicity and comparable efficacy in a phase III trial of pegylated liposomal doxorubicin HCl (CAELYX/Doxil) versus conventional doxorubicin for first-line treatment of metastatic breast cancer. *Ann Oncol* **15**: 440–449.
24. Kim, TY, Kim, DW, Chung, JY, Shin, SG, Kim, SC, Heo, DS *et al.* (2004). Phase I and pharmacokinetic study of Genexol-PM, a cremophor-free, polymeric micelle-formulated paclitaxel, in patients with advanced malignancies. *Clin Cancer Res* **10**: 3708–3716.
25. Winer, EP, Berry, DA, Woolf, S, Duggan, D, Kornblith, A, Harris, LN *et al.* (2004). Failure of higher-dose paclitaxel to improve outcome in patients with metastatic breast cancer: cancer and leukemia group B trial 9342. *J Clin Oncol* **22**: 2061–2068.
26. Blanco, E, Bey, EA, Khemtong, C, Yang, SG, Setti-Guthi, J, Chen, H *et al.* (2010). Beta-lapachone micellar nanotherapeutics for non-small cell lung cancer therapy. *Cancer Res* **70**: 3896–3904.
27. Yamamoto, Y, Nagasaki, Y, Kato, Y, Sugiyama, Y and Kataoka, K (2001). Long-circulating poly(ethylene glycol)-poly(D,L-lactide) block copolymer micelles with modulated surface charge. *J Control Release* **77**: 27–38.
28. Chen, H, Kim, S, He, W, Wang, H, Low, PS, Park, K *et al.* (2008). Fast release of lipophilic agents from circulating PEG-PDLLA micelles revealed by *in vivo* forster resonance energy transfer imaging. *Langmuir* **24**: 5213–5217.
29. Murphy, JE (2011). Clinical Pharmacokinetics. American Society of Health-System Pharmacists: Bethesda.
30. Paál, K, Müller, J and Hegedûs, L (2001). High affinity binding of paclitaxel to human serum albumin. *Eur J Biochem* **268**: 2187–2191.
31. Maeda, H (2001). The enhanced permeability and retention (EPR) effect in tumor vasculature: the key role of tumor-selective macromolecular drug targeting. *Adv Enzyme Regul* **41**: 189–207.
32. Lim, WT, Tan, EH, Toh, CK, Hee, SW, Leong, SS, Ang, PC *et al.* (2010). Phase I pharmacokinetic study of a weekly liposomal paclitaxel formulation (Genexol-PM) in patients with solid tumors. *Ann Oncol* **21**: 382–388.
33. Xiao, K, Luo, J, Li, Y, Lee, JS, Fung, G and Lam, KS (2011). PEG-oligocholic acid telodendrimer micelles for the targeted delivery of doxorubicin to B-cell lymphoma. *J Control Release* **155**: 272–281.
34. Kaminskas, LM, McLeod, VM, Kelly, BD, Sberna, G, Boyd, BJ, Williamson, M *et al.* (2012). A comparison of changes to doxorubicin pharmacokinetics, antitumor activity, and toxicity mediated by PEGylated dendrimer and PEGylated liposome drug delivery systems. *Nanomedicine* **8**: 103–111.
35. Faried, LS, Faried, A, Kanuma, T, Nakazato, T, Tamura, T, Kuwano, H *et al.* (2006). Inhibition of the mammalian target of rapamycin (mTOR) by rapamycin increases chemosensitivity of CaSki cells to paclitaxel. *Eur J Cancer* **42**: 934–947.
36. Haritunians, T, Mori, A, O'Kelly, J, Luong, QT, Giles, FJ and Koeffler, HP (2007). Antiproliferative activity of RAD001 (everolimus) as a single agent and combined with other agents in mantle cell lymphoma. *Leukemia* **21**: 333–339.
37. Campone, M, Levy, V, Bourbouloux, E, Berton Rigaud, D, Bootle, D, Dutreix, C *et al.* (2009). Safety and pharmacokinetics of paclitaxel and the oral mTOR inhibitor everolimus in advanced solid tumours. *Br J Cancer* **100**: 315–321.
38. Sessa, C, Tosi, D, Viganò, L, Albanell, J, Hess, D, Maur, M *et al.* (2010). Phase Ib study of weekly mammalian target of rapamycin inhibitor ridaforolimus (AP23573; MK-8669) with weekly paclitaxel. *Ann Oncol* **21**: 1315–1322.
39. Dong, J, Peng, J, Zhang, H, Mondesire, WH, Jian, W, Mills, GB *et al.* (2005). Role of glycogen synthase kinase 3beta in rapamycin-mediated cell cycle regulation and chemosensitivity. *Cancer Res* **65**: 1961–1972.
40. VanderWeele, DJ, Zhou, R and Rudin, CM (2004). Akt up-regulation increases resistance to microtubule-directed chemotherapeutic agents through mammalian target of rapamycin. *Mol Cancer Ther* **3**: 1605–1613.
41. Sunters, A, Madureira, PA, Pomeranz, KM, Aubert, M, Brosens, JJ, Cook, SJ *et al.* (2006). Paclitaxel-induced nuclear translocation of FOXO3a in breast cancer cells is mediated by c-Jun NH2-terminal kinase and Akt. *Cancer Res* **66**: 212–220.
42. Blanco, E, Bey, EA, Dong, Y, Weinberg, BD, Sutton, DM, Boothman, DA *et al.* (2007). Beta-lapachone-containing PEG-PLA polymer micelles as novel nanotherapeutics against NQO1-overexpressing tumor cells. *J Control Release* **122**: 365–374.
43. Alexis, F, Venkatraman, SS, Rath, SK and Boey, F (2004). *In vitro* study of release mechanisms of paclitaxel and rapamycin from drug-incorporated biodegradable stent matrices. *J Control Release* **98**: 67–74.
44. Sutton, D, Wang, S, Nasongkla, N, Gao, J and Dormidontova, EE (2007). Doxorubicin and beta-lapachone release and interaction with micellar core materials: experiment and modeling. *Exp Biol Med (Maywood)* **232**: 1090–1099.
45. Moreno, A, Akcakanat, A, Munsell, MF, Soni, A, Yao, JC and Meric-Bernstam, F (2008). Antitumor activity of rapamycin and octreotide as single agents or in combination in neuroendocrine tumors. *Endocr Relat Cancer* **15**: 257–266.
46. Saal, LH, Johansson, P, Holm, K, Gruvberger-Saal, SK, She, QB, Maurer, M *et al.* (2007). Poor prognosis in carcinoma is associated with a gene expression signature of aberrant PTEN tumor suppressor pathway activity. *Proc Natl Acad Sci USA* **104**: 7564–7569.
47. Stemke-Hale, K, Gonzalez-Angulo, AM, Lluch, A, Neve, RM, Kuo, WL, Davies, M *et al.* (2008). An integrative genomic and proteomic analysis of PIK3CA, PTEN, and AKT mutations in breast cancer. *Cancer Res* **68**: 6084–6091.
48. Vasudevan, KM, Barbie, DA, Davies, MA, Rabinovsky, R, McNear, CJ, Kim, JJ *et al.* (2009). AKT-independent signaling downstream of oncogenic PIK3CA mutations in human cancer. *Cancer Cell* **16**: 21–32.
49. Pounds, S and Morris, SW (2003). Estimating the occurrence of false positives and false negatives in microarray studies by approximating and partitioning the empirical distribution of p-values. *Bioinformatics* **19**: 1236–1242.
50. Storey, JD (2002). A direct approach to false discovery rates. *J Royal Statistical Society: Series B (Statistical Methodology)* **64**: 479–498.